

1 *Incorporation of HPMCAS during loading of glibenclamide onto mesoporous silica improves dissolution*  
2 *and inhibits precipitation*

3 *Daniel J. Price<sup>1,2</sup>, Anita Nair<sup>1</sup>, Johanna Becker-Baldus<sup>3</sup>, Clemens Glaubitz<sup>3</sup>, Martin Kuentz<sup>4</sup>, Jennifer*  
4 *Dressman<sup>2</sup>, Christoph Saal<sup>1</sup>*

5 <sup>1</sup> *Merck KGaA, Darmstadt, Germany*

6 <sup>2</sup> *Institute of Pharmaceutical Technology, Goethe University Frankfurt, Germany*

7 <sup>3</sup> *Institute for Biophysical Chemistry & Centre for Biomolecular Magnetic Resonance, Goethe University Frankfurt,*  
8 *Germany*

9 <sup>4</sup> *University of Arts and Applied Sciences Northwestern Switzerland, Basel, Switzerland*

10

11 *\*Corresponding Author: Dr Christoph Saal*

12 *Merck KGaA, Site-Management -: Analytics Healthcare*

13 *Frankfurter StraÙer. 250, 64293 Darmstadt (Germany)*

14 *Email: Christoph.saal@merckgroup.com*

15

16 **Keywords:** Mesoporous silica, supersaturation, precipitation inhibition, solid dispersion, mechanistic

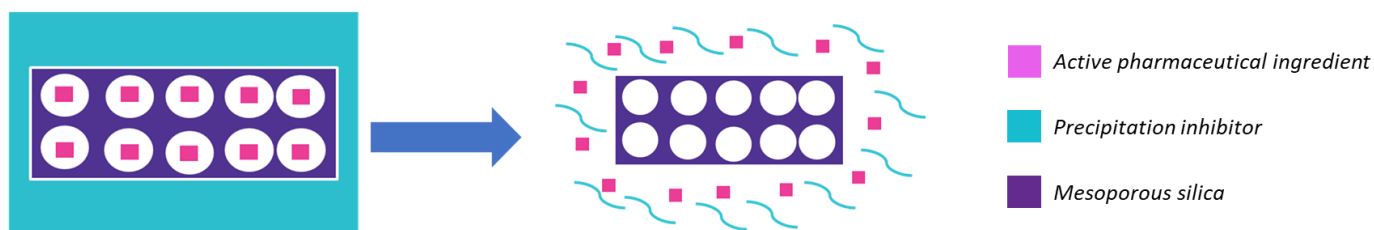
17

18 **Graphical abstract**

19

20

**API/PI Co-loaded Silica Formulations: The Optimal Method for PI Incorporation**



**Solid State and Stomach**

- ✓ Formation of drug-polymer interactions
- ✓ Loaded silica confined to polymer plate
- ✓ No release in stomach

**Intestines**

- ✓ Breakdown of polymer plate
- ✓ Release of supersaturated API
- ✓ Improved precipitation inhibition

21

22

23

24

25

26

27 **Abstract**

28 Mesoporous silica has emerged as an enabling formulation for poorly soluble active pharmaceutical  
29 ingredients (APIs). Unlike other formulations, mesoporous silica typically does not inhibit precipitation of  
30 supersaturated API therefore, a suitable precipitation inhibitor (PI) should be added to increase absorption  
31 from the gastrointestinal (GI) tract. However, there is limited research about optimal processes for  
32 combining PIs with silica formulations. Typically, the PI is added by simply blending the API-loaded silica  
33 mechanically with the selected PI. This has the drawback of an additional blending step and may also not  
34 be optimal with regard to release of drug and PI. By contrast, loading PI simultaneously with the API onto  
35 mesoporous silica, i.e. co-incorporation, is attractive from both a performance and practical perspective.  
36 The aim of this study was to demonstrate the utility of a co-incorporation approach for combining PIs with  
37 silica formulations, and to develop a mechanistic rationale for improvement of the performance of silica  
38 formulations using the co-incorporation approach. The results indicate that co-incorporating HPMCAS with  
39 glibenclamide onto silica significantly improved the extent and duration of drug supersaturation in single-  
40 medium and transfer dissolution experiments. Extensive spectroscopic characterization of the formulation  
41 revealed that the improved performance was related to the formation of drug-polymer interactions  
42 already in the solid state; the immobilization of API-loaded silica on HPMCAS plates, which prevents  
43 premature release and precipitation of API; and drug-polymer proximity on disintegration of the  
44 formulation, allowing for rapid onset of precipitation inhibition. The data suggests that co-incorporating  
45 the PI with the API is appealing for silica formulations from both a practical and formulation performance  
46 perspective.

47

48

49

50

51

52

53

54

55

## 56 **1. Introduction**

57 Among the various administration routes for drugs, oral administration is the most commonly employed.  
58 It is cost-effective and convenient for the patient, leading to a very high patient compliance (Krishnaiah,  
59 2010). APIs must be absorbed to become orally bioavailable, a process which relies in turn on sufficient  
60 solubility and permeability of the API (Zheng, 2012). In recent years there has been an exponential increase  
61 in drugs exhibiting poor solubility: it is reported that approximately 60% of all drugs on the market are  
62 poorly soluble (Taylor and Zhang 2016). It has been suggested that anywhere between 80 and 90% of  
63 compounds in development also demonstrate low solubility (Loftsson, 2010). These estimates highlight  
64 the need for effective formulation approaches to avoid low bioavailability associated with poor aqueous  
65 solubility.

66 To overcome these challenges, formulators have developed a series of promising formulation strategies  
67 (Ditzinger, 2018). These approaches include: (i) solvents, co-solvents and lipids; (ii) micelle systems; (iii)  
68 particle size reduction; (iv) complexation; and (v) amorphous technologies (Zheng, 2012). One of the most  
69 common approaches for improving bioavailability is *via* the generation of supersaturated solutions in the  
70 GI-tract, which can drive improved absorption (Zheng, 2012). However, these systems are metastable due  
71 to the energetic propensity of the compound to precipitate (Price, 2018). Therefore, precipitation  
72 inhibitors (PIs) are often used to sustain the supersaturated state by inhibiting or slowing down  
73 precipitation of drug (Warren, 2010). Successful PI systems can sustain drug supersaturation over  
74 physiologically relevant time-scales by interfering with the crystallization process (Price, 2018).  
75 Precipitation inhibitors can kinetically prevent re-crystallization via a number of mechanisms, including:  
76 viscosity, co-solvency and drug-polymer interactions, with the latter widely being reported to being  
77 especially important (Warren, 2010; Price, 2018). Recent advances in precipitation inhibition design and  
78 selection include *de novo* precipitation inhibitor design (Ting, 2017) and *in silico* calculation of drug-  
79 polymer mixing enthalpies for precipitation inhibitor selection (Price, 2019).

80

81 One under-utilized formulation technology to generate drug supersaturation is mesoporous silica.  
82 Mesoporous silica is a silicon dioxide excipient that has a highly porous network, consisting of mesopores  
83 between 2 and 50 nm in diameter (Barbe, 2009). These materials have very high specific surface areas and  
84 are used in catalysis, environmental clean-up, chromatography, and drug delivery (McCarthy, 2016).  
85 Poorly soluble APIs can become molecularly adsorbed on the surface of the silica and sterically confined  
86 such that recrystallization cannot occur (Knapik, 2016). Indeed, this is one of the most widely reported

87 advantages of mesoporous silica, in its enhanced stabilization capabilities due to nanoconfinement in the  
88 porous network (McCarthy, 2016). Mesoporous silica-based ‘spring and parachute’ formulations have  
89 been widely demonstrated in the literature, from both an *in vitro* and *in vivo* perspective (Ditzinger, 2018;  
90 McCarthy, 2016). Van Speybroeck and colleagues originally described how such precipitation inhibitors,  
91 including HPMC and HPMCAS, can enhance the oral absorption of itraconazole released from mesoporous  
92 silica in rats (Van Speybroeck, 2010). This was also demonstrated in pigs, with O’Shea and colleagues using  
93 the precipitation inhibitor HPMCAS to improve the oral absorption of fenofibrate released from  
94 mesoporous silica (O’Shea, 2016). Recent work on precipitation inhibitors for mesoporous silica has also  
95 taken place, Price and co-workers developed of an *in silico* screening approach which calculates drug-  
96 polymer mixing enthalpy for the optimized selection of precipitation inhibitors for mesoporous silica  
97 formulations (Price, 2019). In spite of these recent advances in mesoporous silica and precipitation  
98 inhibition, the method of combining precipitation inhibitors with mesoporous silica remains relatively  
99 inefficient. Typically, PIs are mechanically blended with the API-loaded silica formulations after the drug is  
100 loaded (usually with a mortar and pestle). However, it has recently been shown that incorporating the PI  
101 into the API loading process itself can dramatically improve both *in vitro* and *in vivo* performance of a  
102 celecoxib loaded silica formulation (Laine, 2016). In light of this proof of concept, there is a need for further  
103 mechanistic research. This study aims to demonstrate the utility of a co-incorporation approach for  
104 combining PIs with silica formulations, and to develop a mechanistic rationale to explain the improvement  
105 in performance of silica formulations using the co-incorporation approach.

106

## 107 **2. Experimental**

### 108 **2.1 Materials**

109 Crystalline glibenclamide (GB), reagent grade acetone, HPLC grade acetonitrile and HPLC grade methanol  
110 were all purchased from MilliporeSigma (St Louis, MO, USA). AQQAT (HPMCAS-MF) was purchased from  
111 ShinEtsu (Japan). Parateck® SLC was a gift sample from Merck KGaA (Germany). FaSSGF/FaSSIF/FeSSIF  
112 powder to make biorelevant dissolution medium, Fasted Simulated Intestinal Fluid (FaSSIF), was obtained  
113 from Biorelevant.com (UK).

### 114 **2.2 Methods**

#### 115 **2.2.1 Determination of thermodynamic solubility**

116 FaSSIF was prepared by weighing 45 mg of FaSSGF/FaSSIF/FeSSIF powder into 45 mL of phosphate buffer  
117 (pH 6.5) (Galia, *et al.* 1998). SGF (pH 1.2) was prepared according to USP monographs. Glibenclamide (2-

118 3mg) was accurately weighed into a Uniprep® syringeless filter (5mL; 0.45µm). 2 mL of either FaSSIF (pH  
119 6.5) or SGF (pH 1.2) was added and the samples were agitated at 450 rpm for 24 hours at 37 °C. The pH  
120 was checked at 7 hours and adjusted with 0.1 N NaOH or 0.1 N HCl, if a deviation greater than +/- 0.05 pH  
121 units was observed. The final pH was also recorded after 24 hours.

122 Samples were filtered with PTFE 0.45 µm Whatman filters after 24 hours. Filtrates were diluted with  
123 acetonitrile and water (1:4) to avoid precipitation from the saturated solution. Samples were analyzed  
124 with ultra-high performance liquid chromatography (UPLC) (Thermo Dionex Ultimate 3000, Thermo Fisher,  
125 MA, USA) to determine the API concentration. API concentration was determined based on a standard  
126 calibration curve of nine standard concentrations (50, 30, 10, 5, 3, 1, 0.5, 0.3, 0.1 µg/mL). Three quality  
127 control samples of known concentrations (30, 3, 0.3 µg/mL) were prepared and used to check the  
128 robustness of the calibration curve. The determination was carried out in duplicate.

### 129 2.2.2 UPLC method

130 UPLC analysis was performed using a Thermo Dionex Ultimate 3000 (Thermo Fisher, MA, USA) equipped  
131 with a diode array detector at 240 nm (Thermo Fisher, MA, USA). Chromatographic separation was  
132 achieved on an Acquity UPLC BEH column C8 (2.1 x 50 mm, 1.7 µm, Waters, MA, USA). The mobile phases  
133 A and B consisted of water: formic acid 99:1 (v:v) and acetonitrile : formic acid 99:1 (v: v), respectively.  
134 Gradient and flow rate is shown in **Table 2**. System management, data acquisition and processing were  
135 performed with the Chromeleon™ software package, version 7.2 (Thermo Fisher, MA, USA)

**Table 2.** UPLC gradient and flow rates

Time (mins)	Flow rate (mL/min)	% (v:v) Mobile phase A	% (v:v) Mobile phase B
0	0.83	90	10
0.83	0.83	10	90
1.2	1.5	90	10
2	1.5	90	10
2.01	0.83	90	10

136

### 137 2.2.3 Parateck SLC® standard loading procedure and standard PI incorporation

138 Glibenclamide loaded silica was prepared using the solvent impregnation rotary evaporator method  
139 (Laine, *et al.* 2016) as follows: A solution (10 mg/mL) of API in acetone was added to Parateck SLC (1:2 w/w  
140 API/Parateck SLC®) under magnetic stirring for 30 minutes. The suspension was then transferred to a rotary

141 evaporator, and the solvent was removed under reduced pressure at 40° C. After complete removal of the  
142 solvent, the powder was left to dry in the rotary evaporator under reduced pressure for a further 2 hours.  
143 The formulation was then physically combined with HPMCAS (API: Parteck SLC®: HPMCAS 1: 2: 3 w/w)  
144 using a pestle and mortar.

#### 145 2.2.4 Parteck SLC® API/PI co-incorporation procedure

146 Glibenclamide/HPMCAS co-incorporated Silica samples were prepared using the solvent impregnation  
147 rotary evaporator method. A solution of API (10 mg/mL) and HPMCAS (30 mg/mL) in acetone was added  
148 to Parteck SLC (1 : 2 : 3 API: Parteck SLC®: HPMCAS) under magnetic stirring, which was continued for 30  
149 minutes. The suspension was transferred to a rotary evaporator, and the solvent was removed under  
150 reduced pressure at 40° C. After complete removal of the solvent, the powder was left to dry in the rotary  
151 evaporator under reduced pressure for a further 2 hours.

#### 152 2.2.5 Preparation of an API-HPMCAS sample as control

153 A control sample consisting of only of API and HPMCAS was also prepared. A solution with the same  
154 concentrations of API (10mg/mL) and HPMCAS (30 mg/mL) as described above for the API – silica – PI  
155 system in acetone was prepared under magnetic stirring for 15 minutes. The solution was then transferred  
156 to a rotary evaporator, and the solvent was removed under reduced pressure at 40° C. After complete  
157 removal of the solvent, the powder was left to dry in the rotary evaporator under reduced pressure for a  
158 further 2 hours. Residual solvent concentration was recorded with 2D <sup>1</sup>H NMR to ensure residual solvent  
159 was below the ICH limit of 0.5% (data not shown).

#### 160 2.2.6 Determination of glibenclamide loading onto mesoporous silica

161 To determine the % (w/w) of API in the mesoporous silica, the loaded samples were dispersed and stirred  
162 in DMSO as this solvent is known to dissolve glibenclamide readily. Samples were taken after 1 hour,  
163 centrifuged, filtered and diluted before being quantified by UPLC, according to the method described in  
164 2.2.2. The API content was calculated relative to the mass of loaded samples dispersed within the DMSO.  
165 The study was performed in triplicate.

#### 166 2.2.7 Powder X-Ray Diffraction (PXRD)

167 Samples were prepared between X-ray amorphous films and measured in transmission mode using Cu-  
168 K $\alpha$ 1-radiation and a Stoe StadiP 611 KL diffractometer equipped with Dectris Mythen1K PSD. The  
169 measurements were evaluated with the software WinXPow 3.03 by Stoe, Crystallographica Search/Match  
170 Version 3.1.0.2, the ICDD PDF-4+ 2014 Database and Igor Pro Version 6.34 by Wavemetrics Inc.

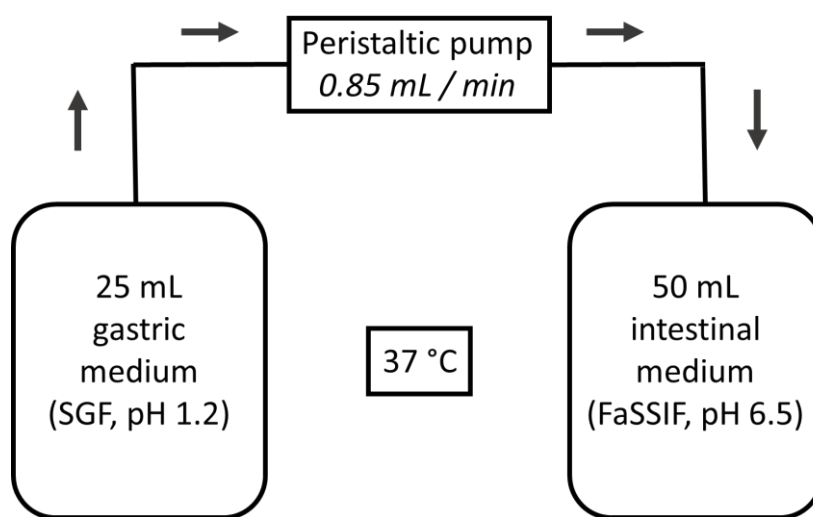
171 Finger/Cox/Jephcoat. Angular range: 1-65 °2θ; PSD-step width: 2 ° 2 θ; angular resolution: 0.015 °2θ  
172 measurement time: 15 s/step, 0.25 h overall.

### 173 2.2.8 FaSSIF mini-dissolution experiment

174 Around 5 mg of API (or the equivalent of API-loaded silica) was weighed accurately into a glass vial. 5 mL  
175 of FaSSIF was added. The vials were agitated at 37 °C and 450 rpm in a shaker for 2 hours. Samples were  
176 taken at 2, 15, 60 and 120 minutes, filtered (0.45 PTFE Whatman filters), diluted, and analyzed by UPLC.  
177 Solid residues at the end of the experiment were collected *via* centrifugation and analyzed for crystallinity  
178 with powder X-ray diffraction (PXRD). This was carried out on the following samples: API, API + polymer,  
179 API loaded silica and API loaded silica + PI. The mini-dissolution trials were conducted in duplicate for all  
180 samples.

### 181 2.2.9 Biorelevant transfer experiments

182 The experimental set-up for the transfer experiments is demonstrated in **Figure 1**.



183

184

185 **Figure 1.** Experimental diagram showing mini-transfer set-up

186 Around 150 mg of API or equivalent was accurately weighed in a 100 mL stoppered flask - the exact sample  
187 masses varied dependent on the formulation (*see Table 1*).

**Table 1. Transfer dissolution sample preparation**

<b>Formulation</b>	<b>Weighed mass (mg)</b>	<b>API mass (mg)</b>
--------------------	--------------------------	----------------------

<b>GB loaded silica</b>	450	150
<b>GB loaded silica HPMCAS Blend</b>	900	150
<b>GB and HPMCAS co- incorporated silica</b>	900	150

188  
189 25mL of simulated gastric fluid (pH 1.2) prepared according to USP monographs was added to the flask  
190 and agitated at 450 rpm and 37 °C. 50mL of FaSSIF were added to a separate flask, which was also agitated  
191 at 450 rpm and 37 °C. After 30 minutes, the API suspension in SGF pH 1.2 was transferred at a zero-order  
192 rate of 0.85 mL/min using a peristaltic pump, until the complete gastric contents were transferred (~30  
193 minutes) into the FaSSIF compartment. Samples were withdrawn from the intestinal compartment at  
194 regular time points using a 1 mL syringe to a sampling tube fitted with a pre-filter of 10 µm and filtered  
195 again using a 0.45 µm PTFE Whatman syringe filter and diluted. Samples were then analyzed by UPLC for  
196 API content. The post-dissolution residues were then collected and analyzed for crystallinity with XRPD.

197 2.2.10 Single medium SGF dissolution assay (in tandem to transfer assay)

198 Around 150 mg of API or equivalent was accurately weighed into a 100 mL stoppered flask. The exact  
199 sample masses varied dependent on the formulation (*see Table 1*). 25mL of SGF (pH 1.2, gastric  
200 compartment) was added to the flask and the contents agitated at 450 rpm and 37 °C. Samples were  
201 withdrawn at regular time points using a 1 mL syringe to a sampling tube fitted with a pre-filter of 10 µm  
202 and filtered again using a 0.45 µm PTFE Whatman syringe filter and suitably diluted. Samples were then  
203 analyzed with UPLC for API content. The post-dissolution residues were directly collected and analyzed  
204 for crystallinity with PXRD.

205 2.2.11 Scanning Electron Microscopy (SEM) and Energy-Dispersive X-ray Spectroscopy (EDX)

206 Samples were prepared on copper tape and imaged using a Hitachi TM3000 Tabletop Microscope, W  
207 cathode, low vacuum, accelerating voltage 5 kV and 15 kV, 4-Quadrant BSE detector, magnification 15x –  
208 30,000x. For the energy dispersive X-ray spectroscopy (EDX) data, a standard-less quantitative analysis was  
209 performed by using the ZAF correction, considering the correction for light elements standardless element  
210 coefficient factors (SEC).

211 2.2.12 Solid-state Nuclear Magnetic Resonance (NMR) spectroscopy

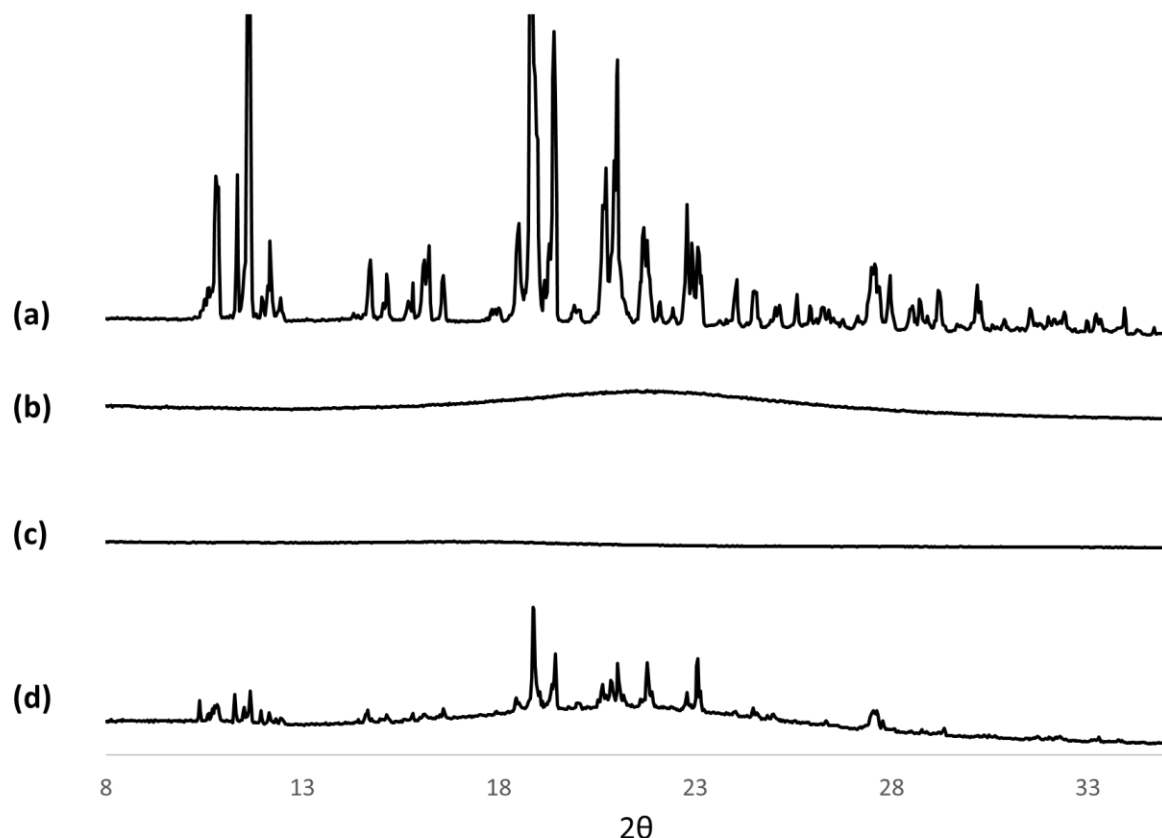


212 Solid-state NMR experiments were performed under magic-angle-sample (MAS) spinning using a Bruker 4  
213 mm MAS HXY probe in double resonance mode in combination with a Bruker Avance 600 MHz wide bore  
214 NMR spectrometer (Bruker). The sample spinning frequency was 10 kHz, and the readout on the probe  
215 thermocouple was set to 290 K. <sup>13</sup>C-CP experiments were performed using a contact time of 1 ms and 100  
216 kHz high power proton decoupling following the SPINAL64 scheme was applied during acquisition. The  
217 recycle delay was 3 s. The spectra were indirectly referenced to DSS via the CH<sub>2</sub> signal of Adamantane at  
218 40.49 ppm. Solid-state NMR measurements were repeated on multiple batches to ensure reliability of the  
219 interpretation.

## 220 **3. Results**

### 221 **3.1 Solid-state form of glibenclamide in formulations**

222 The glibenclamide powder used in this work is crystalline in the solid-state as shown by XRPD (**Figure 2a**).  
223 Successful loading of glibenclamide onto mesoporous silica was demonstrated by the absence of distinct  
224 Bragg peaks in XRPD patterns, which indicated a shift from the crystalline to the amorphous state (**Figure**  
225 **2b**). The co-incorporation process did not interfere with the solid-state conversion of glibenclamide: the  
226 co-incorporated sample exhibited the same shift from crystalline to amorphous post-loading (**Figure 2c**).  
227 However, the control sample, which consisted of HPMCAS/GB prepared by solvent evaporation, showed  
228 partial crystallinity, which aligned with the XRPD pattern for the unmodified crystalline glibenclamide  
229 (**Figure 2d**).



230  
 231 **Figure 2.** XRPD pattern for crystalline glibenclamide (GB) (a), glibenclamide loaded silica (b), GB and  
 232 HPMCAS co-incorporated silica (c) and GB and HPMCAS prepared by rotary evaporation (d)

233  
 234 **3.2 Loading content of glibenclamide in mesoporous silica formulations**

235 The % loading of glibenclamide determined by UPLC is shown in **Table 3**. The final glibenclamide content  
 236 in the final mesoporous silica formulations was around 15%, irrespective of whether the drug was first  
 237 loaded onto the silica and then combined with HPMCAS, or the HPMCAS was incorporated during drug  
 238 loading. Drug loading levels are modest, which could be a limitation for drugs that are administered at  
 239 high doses. However, they are in line with usual supersaturating drug formulations that require  
 240 precipitation inhibitors (Price, 2019; Ditzinger, 2018).

241

**Table 3. API loaded silica total API content**

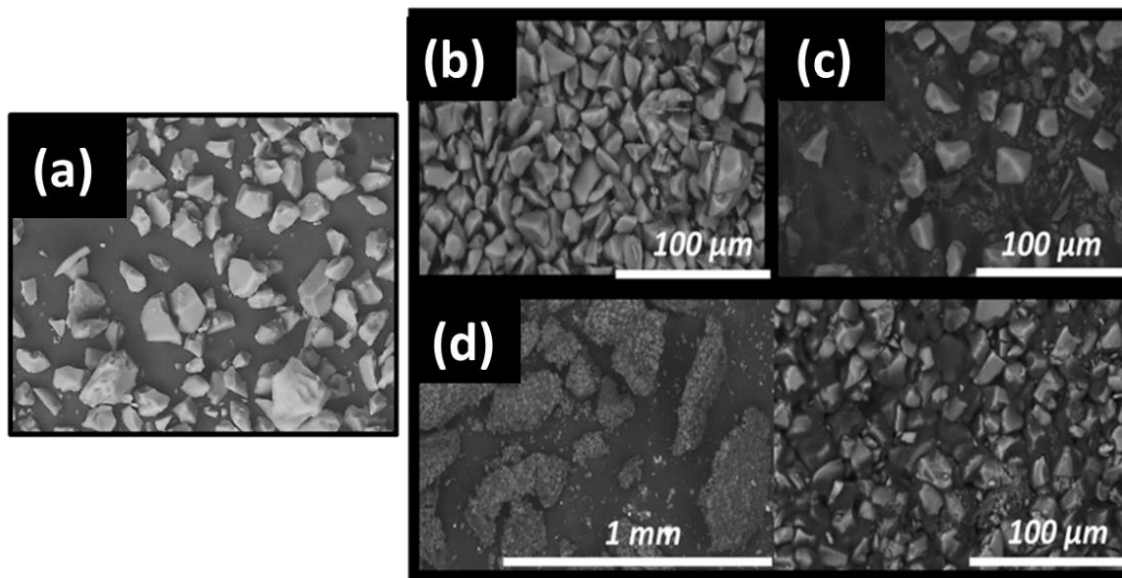
Formulation	Theoretical loading (%)	Actual loading (UPLC) (%)
-------------	-------------------------	---------------------------

Glibenclamide loaded silica (without HPMCAS)	30	30.1 ± 0.1
Glibenclamide and HPMCAS co-incorporated silica	15	15.9 ± 0.2
Glibenclamide loaded silica + HPMCAS blend	-	15.1

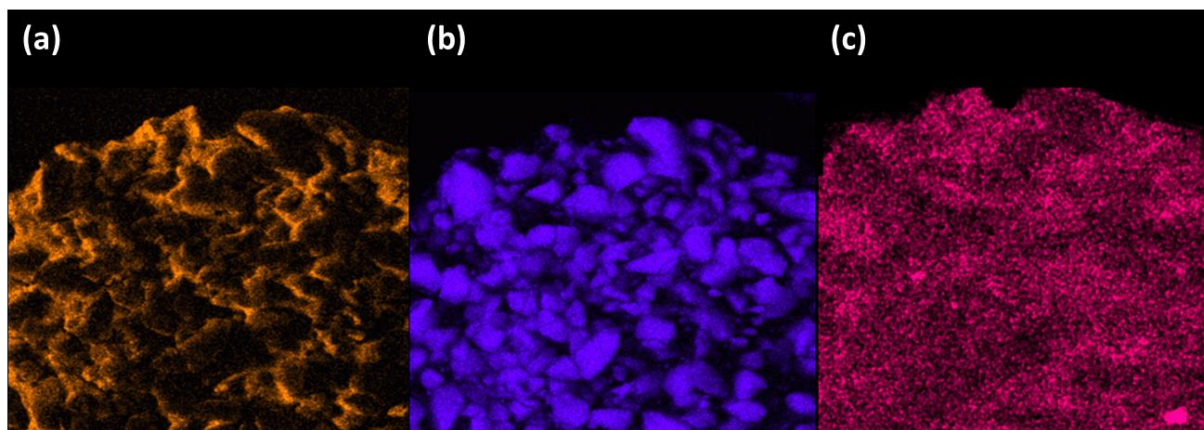
242

243 **3.3 Scanning Electron Microscopy (SEM) and Electron Dispersive X-ray Spectroscopy (EDX)**

244 SEM images for glibenclamide loaded silica, glibenclamide loaded silica + HPMCAS Blend and SEM and EDX  
 245 images for glibenclamide and HPMCAS co-incorporated silica are shown in **Figure 3**. The unloaded silica is  
 246 shown in Figure 3a. In glibenclamide loaded silica, the characteristic silica particles are also present (**Figure**  
 247 **3b**). This is also the case for glibenclamide loaded silica + HPMCAS physical mixture (**Figure 3c**), where the  
 248 particles are simply ‘diluted’ by the addition of the polymer, which is depicted as the dark texture in  
 249 between the silica particles. However, large platelet particles were observed when HPMCAS was  
 250 incorporated during the loading step onto the silica (**Figure 3d**). The EDX images show that the platelet  
 251 particles are carbon based and therefore likely composed of HPMCAS. The silica particles appear to be  
 252 embedded in the HPMCAS plate, as when the image was zoomed to the same resolution as **Figures 3**, the  
 253 images looked similar to characteristic silica particles. Chlorine, used as a marker for glibenclamide, was  
 254 observed within the silica particles on the HPMCAS plate, with no API observable outside of the platelets.  
 255 These observations suggest that the formulation is a solid dispersion of API loaded silica in HPMCAS (Figure  
 256 3 bottom).



257



258

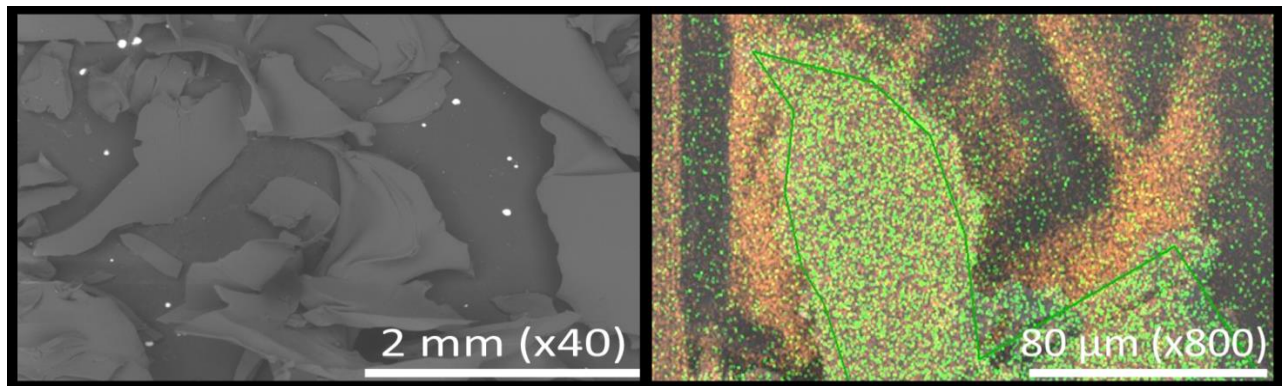
259

260 **Figure 3.** Top: SEM (left) of unloaded mesoporous silica (a), glibenclamide loaded silica (b), glibenclamide  
 261 loaded silica + HPMCAS physical mixture (c) and HPMCAS incorporated during loading of glibenclamide  
 262 onto silica (d).

263 Bottom: SEM EDX of HPMCAS incorporated during loading of glibenclamide onto silica. Carbon (a), silicon  
 264 (b) and chlorine (c) atoms are highlighted. Chlorine is a marker for glibenclamide.

265 Based on this potential combination of silica loading and classical solid dispersion, it was important to  
 266 assess what role the silica plays in the formulations. As can be seen in Figure 4, the particles produced in  
 267 the solvent evaporation of glibenclamide and HPMCAS (control sample) are similar to the particles  
 268 produced when the HPMCAS is incorporated during the drug loading step onto the silica. However, EDX

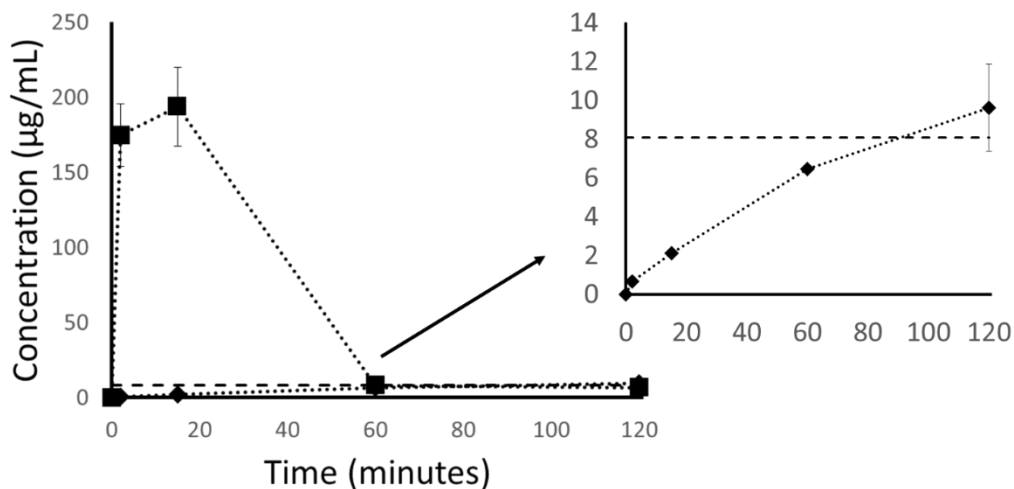
269 analysis shows a key difference between the formulations, in that the drug marker, chlorine, is no longer  
270 confined within the polymer (plates), but is freely distributed in the control sample.



272 **Figure 4.** SEM (left) and EDX (right) images of glibenclamide and HPMCAS prepared by solvent evaporation  
273 shows the same particle size and morphology as the co-incorporated samples. However, in this sample the  
274 drug (indicated by green) is no longer confined within the polymer plate and is freely distributed  
275 throughout the sample.

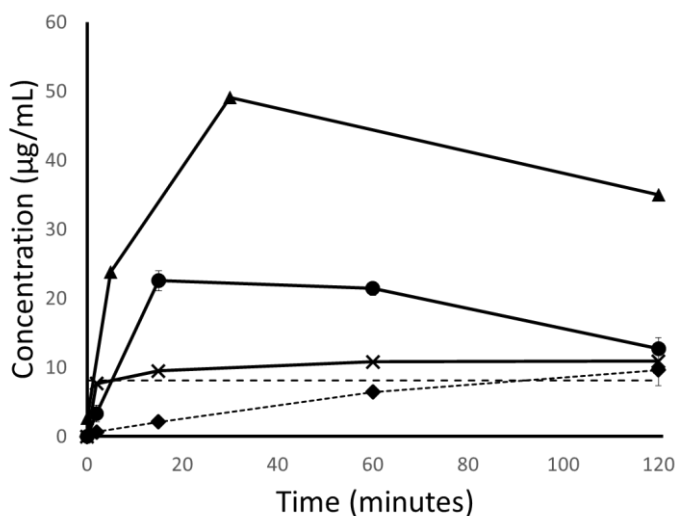
### 276 3.4 FaSSIF mini-dissolution

277 In FaSSIF mini-dissolution experiments, the concentration of the pure drug approached the  
278 thermodynamic solubility value of 8.1  $\mu\text{g/mL}$  (**Appendix 1**) (**Figure 5a**). From the glibenclamide loaded  
279 silica formulations, a significant improvement in dissolution was observed in the FaSSIF mini-dissolution  
280 experiments, reaching a 25-fold supersaturation (**Figure 5**). However, due to the metastable nature of the  
281 supersaturation, these extremely high concentrations were short-lived and the concentration reverted to  
282 the thermodynamic solubility within 60 minutes (**Figure 5**).



284 **Figure 5.** Mini-dissolution profiles of glibenclamide (◆), and glibenclamide loaded silica (▪) in FaSSIF, pH 6.5  
285 at 37°C (n=2). Mean Glibenclamide thermodynamic solubility in FaSSIF is represented by the dashed  
286 horizontal line. In the insert on the right, the dissolution of crystalline glibenclamide has been magnified  
287 for better comparison.

288 Physically blending the glibenclamide loaded silica with HPMCAS prolonged the duration of  
289 supersaturation to at least 2 hours, although the degree of supersaturation was lower (about 3-fold)  
290 **(Figure 6)**. Co-incorporating the HPMCAS with the glibenclamide onto the silica further improved the  
291 dissolution and precipitation performance, with higher supersaturation (about 6–fold) achieved over the  
292 time course of the experiment **(Figure 6)**. Finally, the control sample, which used the same process as the  
293 co-incorporated in the absence of silica, showed almost no improvement in the FaSSIF mini-dissolution  
294 relative to the crystalline API. This result is in agreement with the partial crystallinity observed in the XRPD  
295 **(Figure 6)**.



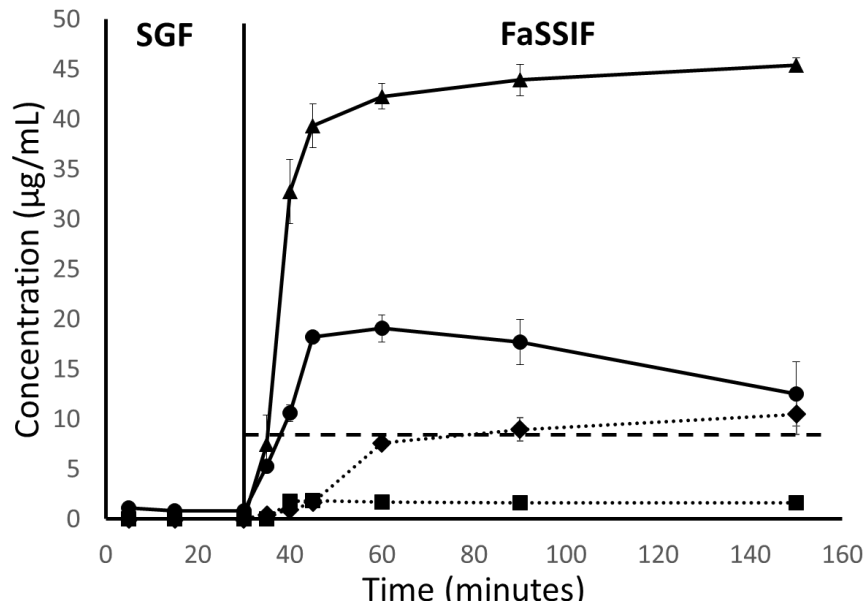
296 **Figure 6.** Mini-dissolution profiles of glibenclamide (◆), glibenclamide loaded silica + HPMCAS blend (●)  
297 and glibenclamide and HPMCAS Co-incorporated silica (▲) and control: glibenclamide/HPMCAS prepared  
298 by solvent evaporation (X) in FaSSIF, pH 6.5 at 37°C (n=2).  
299

300 Post-dissolution residues were collected for each of the samples and analyzed by XRPD. Crystalline  
301 glibenclamide precipitated in all samples except the co-incorporated formulation, in which the solid  
302 residue at the end of the experiment was amorphous **(Appendix 2)**.

### 303 3.5 Transfer model experiments

304 During transfer model dissolution experiments with pure glibenclamide, no concentrations were detected  
305 in the SGF portion of the assay (**Figure 7**). This is in line with the thermodynamic solubility results, which  
306 indicated that the solubility of glibenclamide was under the limit of detection of the UPLC method  
307 (**Appendix 1**). After transfer into the FaSSIF portion of the experiment, the concentration profile closely  
308 overlapped with the mini-dissolution profile, suggesting that the dissolution of crystalline glibenclamide  
309 was largely unaffected by pre-wetting in SGF (**Figure 7**).

310 Comparison of results from transfer model and mini-dissolution experiments of glibenclamide loaded silica  
311 in the absence of any precipitation inhibitors suggests that single-medium dissolution may lead to different  
312 expectations of formulation performance. In the transfer model experiments with glibenclamide loaded  
313 silica (**Figure 7**); the performance of the loaded silica formulation was even poorer than the unmodified,  
314 crystalline parent.



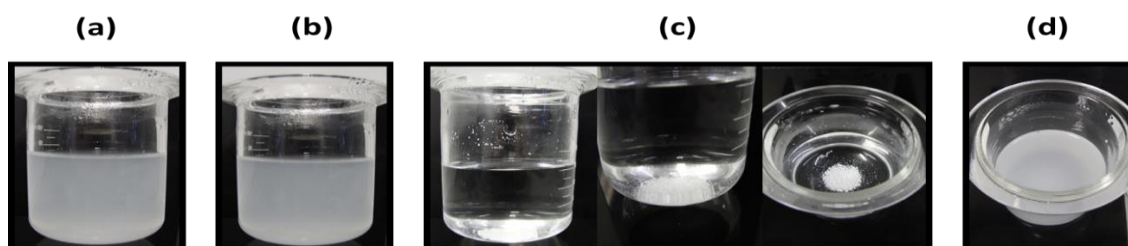
315 **Figure 7.** Biorelevant transfer dissolution of glibenclamide loaded silica (▲), crystalline glibenclamide (◆),  
316 glibenclamide Loaded Silica + HPMCAS Blend (●) and glibenclamide and HPMCAS co-incorporated silica (▲  
317 ) (n=2). Transfer from SGF to FaSSIF occurred at 30 minutes. N.B. no API was detectable during the SGF  
318 dissolution for glibenclamide loaded silica and crystalline glibenclamide. FaSSIF thermodynamic solubility  
319 is shown by the dotted line.  
320

321 Crystallinity was observed in the post-SGF dissolution residues for glibenclamide loaded silica (**Appendix**  
322 **3**). This suggests that, although no release was detectable in SGF, the drug did indeed release but then  
323 rapidly precipitated to the crystalline form.

324 Combination of glibenclamide loaded silica with HPMCAS significantly improved the transfer dissolution  
325 performance, with the formulation generating supersaturation in the intestinal phase of the assay (**Figure**  
326 **7**). It was also possible to detect glibenclamide in the SGF portion of the assay, suggesting that  
327 supersaturation occurred in this medium. Similarly to the glibenclamide loaded silica, crystallinity was  
328 observed in the post-SGF residue for the sample containing a physical mixture of HPMCAS with the drug  
329 loaded silica (Appendix 3). This finding was in agreement with the XRPD patterns obtained post-FaSSIF  
330 mini-dissolution (Appendix 2).

331 The transfer dissolution of the sample where HPMCAS was incorporated during the drug loading step is  
332 shown in Figure 7. Unlike the sample where HPMCAS was added post-loading, no release of glibenclamide  
333 was observed in the SGF of the portion of the assay. This is likely explained by the immobilization of the  
334 drug loaded silica onto the HPMCAS platelets, which do not disintegrate in the gastric environment. As  
335 observed in the mini-dissolution experiments, (i) the supersaturation of glibenclamide during the FaSSIF  
336 portion of the experiment was significantly greater and more sustained from the co-incorporated  
337 formulation compared to the blend. In this case (unlike the pure drug ), similar concentrations were  
338 achieved in the mini-dissolution and transfer model experiments.

339 Visually, the transfer dissolution of the sample in which HPMCAS was incorporated during the drug loading  
340 step was also quite different from the glibenclamide loaded silica and physical mixture of glibenclamide  
341 loaded silica with HPMCAS samples. For glibenclamide loaded silica with and without post-loading  
342 addition of HPMCAS, the powder was immediately dispersed in the dissolution vessel, creating a  
343 suspension. Conversely, no such dispersion was observed within the sample in which HPMCAS was  
344 incorporated in the drug loading step and the dispersion remained clear (Figure 8).



345  
346 **Figure 8.** Images of glibenclamide loaded silica (a) and glibenclamide loaded silica + HPMCAS (b) dispersed  
347 in SGF; and glibenclamide and HPMCAS co-incorporated silica dispersed in SGF (c) and FaSSIF (d)

348 Unlike the other silica formulations, the post-SGF dissolution residue for the co-incorporated formulation  
349 remained amorphous (**Appendix 3**).

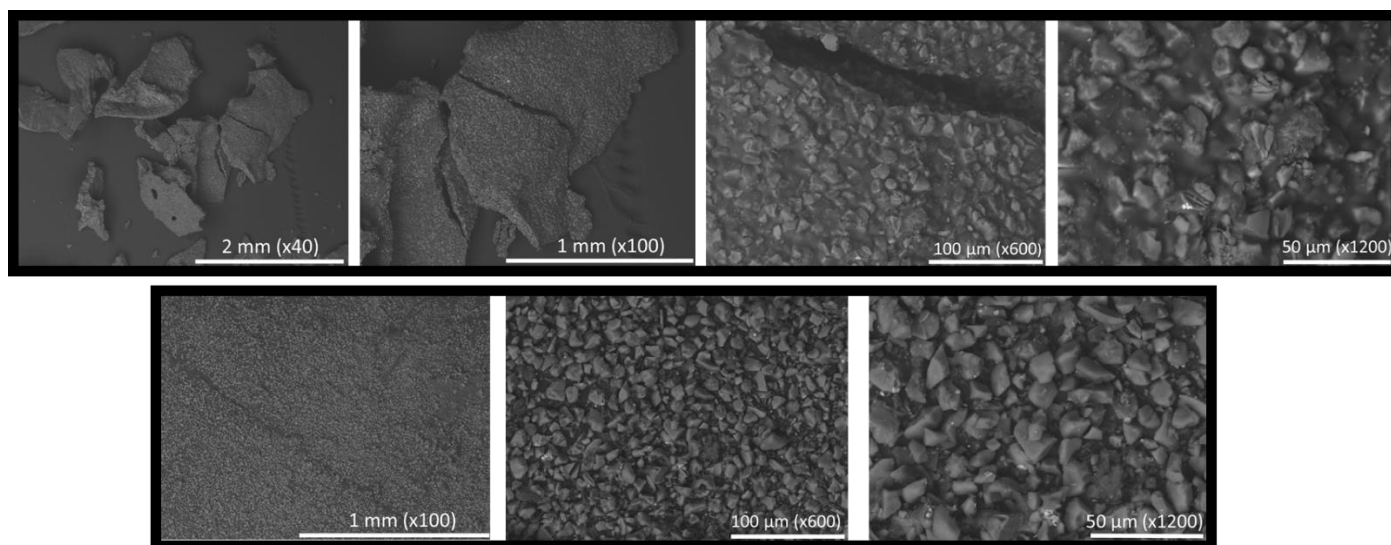


350 The control sample was not investigated during the transfer dissolution as it was fully crystalline and  
351 behaved identically to pure crystalline glibenclamide during dissolution in FaSSIF. Furthermore, given that  
352 the thermodynamic solubility of crystalline glibenclamide is < LOD it was not anticipated that any useful  
353 observations could be made from the control sample during the SGF portion of the transfer dissolution.

### 354 3.2.6. Post-dissolution SEM

355 To examine the physical behavior of the formulation with HPMCAS incorporated during the drug loading  
356 step, the post-SGF and post-FaSSIF residues were characterized with SEM. Post-SGF dissolution, the large  
357 platelets (Figure 3) were unchanged (Figure 9). Increasing the magnification, one can still observe the  
358 loaded silica particles immobilized within the polymer platelets. Conversely, in post-FaSSIF dissolution, the  
359 only observable particles are of silica, suggesting the polymer platelets had dissolved, allowing the drug to  
360 be released from the silica (Figure 9)

361

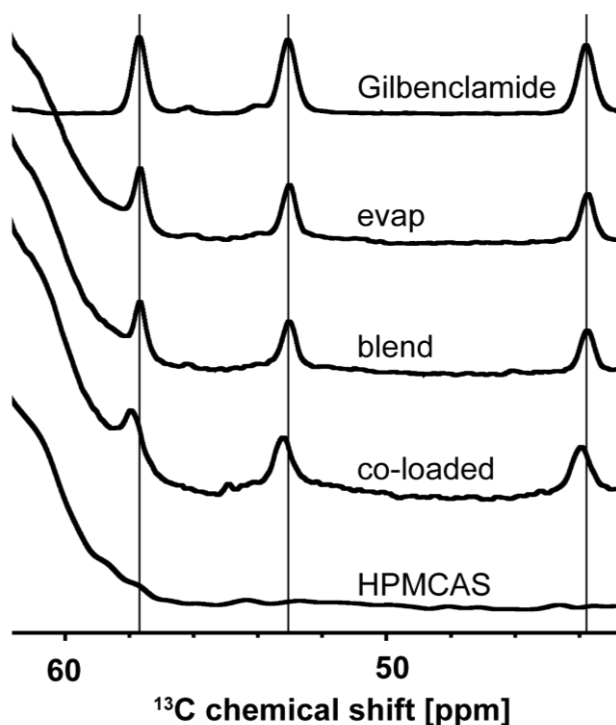


362  
363 **Figure 9.** SEM images of glibenclamide and HPMCAS co-incorporated silica after dissolution in SGF (top)  
364 and FaSSIF (bottom)

### 365 3.2.7 Solid-state NMR spectroscopy

366 SS-NMR spectroscopy was carried out on all samples (**Figure 10**). The full spectra are provided in **Appendix**  
367 **4**. The <sup>13</sup>C peaks for the API were identical in all samples except the co-incorporated formulation. In the  
368 co-incorporated formulation, a low field shift of 0.2 – 0.3 ppm for all API peaks was observed. For example,  
369 the characteristic API peak at 53 ppm was observable in all samples except the co-incorporated  
370 formulation, in which the peak shifted to 53.5 ppm. This is indicative of an interaction taking place between

371 the drug and the polymer in the solid-state, which can take place once the drug is immobilized in the silica  
372 and subsequently in the HPMCS plate. By contrast, no peak shift was observed in the control sample,  
373 GB/HPMCAS, which was prepared by rotary evaporation. The results suggest that solid-state drug-polymer  
374 interactions and hence dissolution performance can be altered by changing the method used to  
375 manufacture the formulation.



376  
377 **Figure 10.** A section of the  $^{13}\text{C}$  NMR spectra for all samples showing characteristic peaks for API  $^{13}\text{C}$  atoms  
378 at 43.5, 53 and 58 ppm. Analysis was carried out on multiple batches ( $n=2$ ) of co-incorporated formulation  
379 and in all cases a 0.2 - 0.3 ppm peak-shift was observed for the co-incorporated formulation versus all other  
380 samples, with the co-incorporated formulation showing API  $^{13}\text{C}$  peaks at 44, 53.5 and 58.5 ppm. Given that  
381 the spectra were unchanged for different batches and repeats, only one dataset is show. Full spectra are  
382 available in **Appendix 4**.

#### 383 **4. Discussion**

384 Mesoporous silica is an emerging oral delivery technique to formulate low soluble drugs. Upon  
385 impregnation of the silica with a concentrated API solution, drug can be molecularly adsorbed onto the  
386 surface of the silica. Due to the size of the pores, which have an approximate mean diameter of 4 nm, the  
387 molecularly adsorbed API is locally and sterically confined, preventing recrystallization (Ditzinger, Price,

388 2018). More understanding is required to fully resolve the relative importance of the various  
389 considerations in the design and development of mesoporous silica formulations. Particularly critical is  
390 incorporation of precipitation inhibitors in the final formulation, since without such additives, the  
391 supersaturated state of the API is barely stabilized.

392 To date there has been no systematic study of how best to incorporate precipitation inhibitors in  
393 mesoporous silica formulations. Current practice for preparation on a small scale involves combining PIs  
394 in a physical mixture with the API loaded silica, either by mortar and pestle or overhead stirring. Due to  
395 the lack of a standard protocol, there is uncertainty about the reliability of this approach and how well the  
396 PI is blended with the loaded silica. In addition to the practical limitations of incorporating the PI post-  
397 loading, it represents a further step in product manufacture. By contrast, incorporation of the PI during  
398 the loading step removes these limitations while maintaining improvement in dissolution of the API. Laine  
399 and co-workers demonstrated that incorporation of HPMCAS during loading of celecoxib onto mesoporous  
400 silica substantially improved both the *in vitro* and *in vivo* performance of this poorly soluble API (Laine,  
401 2016). In the current study, we have not only demonstrated a marked improvement in dissolution of the  
402 BCS II compound, glibenclamide, by the co-incorporation approach, but have additionally proposed a  
403 mechanistic hypothesis of how this enhanced performance is achieved.

#### 404 **Understanding the effect of adsorption onto mesoporous silica on release in a transfer experiment**

405 In the current study, a successful conversion of glibenclamide to the amorphous form after loading onto  
406 mesoporous silica was confirmed with XRPD. This conversion led to 25-fold supersaturation during FaSSIF  
407 mini-dissolution (**Figure 2b** and **Figure 5**). Given the instability of the supersaturated state, the system  
408 rapidly precipitated and returned to its thermodynamic solubility, in line with previous studies with  
409 mesoporous silica (McCarthy, 2016; Laine, 2016; Price, 2019). Although precipitation was observed in the  
410 single-medium FaSSIF dissolution test, the full effect of precipitation on the overall performance was only  
411 realized by considering transfer dissolution data. In these experiments, no dissolution of crystalline  
412 glibenclamide (i.e. pure API) was observed in SGF, because its thermodynamic solubility is below the limit  
413 of detection at this pH. By contrast, in the transfer dissolution of the supersaturating silica formulation,  
414 API was detected in the SGF phase, suggesting that supersaturation occurred (**Figure 7**). This  
415 supersaturation of API in the SGF portion of the assay allowed precipitation to commence, along with the  
416 generation of seed crystals. This resulted in significantly poorer dissolution performance of the API-silica  
417 formulation in the FaSSIF portion of the experiment, relative to the single-medium approach (**Figure 7**).  
418 Therefore, one should consider the effect of transfer from the stomach to the intestine when assessing

419 the dissolution performance of supersaturating formulations, especially mesoporous silica-based  
420 formulations.

421

#### 422 **Application of HPMCAS as a precipitation inhibitor: blending vs. co-incorporation**

423 For the current study, HPMCAS was selected as model precipitation inhibitor. HPMCAS is a well-established  
424 PI and has a track record in the literature of successfully sustaining supersaturated solutions for a range of  
425 APIs (Warren, 2010; Price, 2018; Laine, 2016; Udea, 2015).

426 From a practical perspective, the co-incorporation of precipitation inhibitor in the same formulation step  
427 is appealing, however, one potential concern for the co-incorporation approach is the accessibility of the  
428 pores for the API so that adsorption and nanoconfinement can still occur (Laine, 2016). Encouragingly, co-  
429 incorporating HPMCAS with glibenclamide onto mesoporous silica successfully converted the solid-state  
430 form of the API from the crystalline to the amorphous phase. This is in line with previous experience with  
431 celecoxib (Laine, 2016). Previous literature, which describes the incorporation of a polymer into the  
432 loading process as a “co-load” might infer the adsorption of the polymer inside the porous network.  
433 However, the molecular weight of the HPMCAS polymer used is approximately 18,000 Da. This is 36-times  
434 larger than the API, glibenclamide, which has a molecular weight of 484 Da. Given the very small size of  
435 the pore, 6 nm in diameter, it is highly unlikely that the polymer is actually co-loaded inside the pore.  
436 Further, the particles in samples where HPMCAS has been incorporated into the formulation appear to be  
437 larger and different in shape than API-loaded silica samples without HPMCAS (Figure 3) data confirmed  
438 that these plate-like particles were composed of carbon and, therefore, it was concluded that the plate-  
439 like particles were comprised of HPMCAS.

440 The next important consideration, on the location of the API within the formulation, was addressed with  
441 EDX spectroscopy. EDX is a useful tool to envisage the distribution of a drug within a formulation. In the  
442 samples where HPMCAS was incorporated during the drug loading step, it was observed that drug was  
443 adsorbed onto the mesoporous silica particles and partly within the HPMCAS plate. Crucially, there was  
444 no API observed outside of these newly present HPMCAS plates. Therefore, it was concluded that co-  
445 incorporating the PI resulted in a solid dispersion of glibenclamide as the loaded silica. This appears to be  
446 the first example of such a solid dispersion in the literature. Given the novelty of this system, further work  
447 should be carried out to investigate the solid-state stability of the amorphous API in the system, which is  
448 an essential consideration for amorphous formulations (Ditzinger, 2018). Specifically, future work is

449 planned to assess the amorphous stability of the API in the formulation, in line with the ICH Q1 conditions  
450 for accelerated stability.

451 Neither the formulation in which HPMCAS was incorporated during the loading step nor the sample where  
452 it was added post-loading was able to capture the extremely high 25-fold supersaturation generated by  
453 simply loading the drug onto the silica. However, it has often been observed that the efficiency of  
454 precipitation inhibition is not able to capture the full supersaturation potential generated by the enabling  
455 formulation alone (Price, 2018; Price 2019). In spite of this, it was observed that when HPMCAS was  
456 incorporated during rather than after the drug loading step, the dissolution profile was much higher.  
457 Addition of HPMCAS post-loading improved the performance of glibenclamide loaded silica during both  
458 single-medium and transfer dissolution experiments, but there was some evidence of re-crystallization,  
459 suggesting that in a simple physical mixture HPMCAS is not able to completely inhibit precipitation. Indeed,  
460 incorporating the HPMCAS during the drug loading step demonstrated a 3-fold enhancement in dissolution  
461 performance compared to the simple physical mixture (Figure 6 and Figure7). Such an improved  
462 precipitation inhibition effect could be related to the formation of drug polymer interactions already in  
463 the solid-state, which appears to be crucial for maximum precipitation inhibition (Price, 2018). This was  
464 supported by solid-state NMR data, in which a peak-shift was observed for co-incorporated formulations  
465 but not for other samples (**Figure 10**). Although the peak-shift was small (0.2 – 0.3 ppm), it was consistently  
466 observed for different batches. Alternative methods for obtaining information about drug-polymer  
467 interaction, for example 2D NOESY NMR, were unsuccessful because sufficiently concentrated solutions  
468 of drug-polymer could not be achieved. Another potential mechanism for enhanced precipitation  
469 inhibition in the formulation in which HPMCAS was incorporated during the drug loading step is the  
470 generation of an increased viscosity in the microenvironment surrounding the dissolving plates in FaSSiF.  
471 Such an increased viscosity would decrease the diffusion time out of the formulation and allow drug and  
472 polymer to remain in close proximity, both of which have been shown to be crucial factors in nucleation  
473 time in the presence of precipitation inhibitors (Price, 2018; Warren, 2010). However, further work would  
474 be required to fully confirm this hypothesis.

475

476 During the transfer experiment, it was observed that the HPMCAS plates do not disperse in SGF (**Figure 8**).  
477 This is a significant benefit, given that the HPMCAS plates did not break down, the API-loaded silica  
478 remained immobilized and API could not be released from the silica. Therefore, the formation of seed  
479 crystals in SGF was prevented. Ultimately, this has a significant effect on the dissolution performance and  
480 provides an additional mechanism by which formulations with HPMCAS incorporated during the drug

481 loading step can improve dissolution performance. In addition, it is interesting to observe that a change in  
482 manufacturing process - without a change in the qualitative and quantitative composition of the  
483 formulation - can introduce new properties to the product. By incorporating the HMPCAS during the  
484 loading step rather than post-loading, premature release of the drug from the formulation was  
485 circumvented without the need to add extra excipients, coating processes or special capsules, which are  
486 typically otherwise required (Qiu and Lee, 2017). This property should be especially advantageous in the  
487 delivery of poorly soluble basic compounds, whose premature release and supersaturation in the stomach  
488 (due to ionization in acidic conditions) with subsequent precipitation in the intestine could be avoided.  
489 Although Van Speybroeck and colleagues described an improved oral absorption of itraconazole loaded  
490 silica in rats, they found that silica formulations with post-loading incorporation of HMPCAS were were  
491 unable to prevent the release of API in the stomach and therefore absorption was reduced (Van  
492 Speybroeck, 2010). The potential for incorporation of HMPCAS during the drug loading step on the  
493 dissolution performance of poorly soluble weak base drugs should be further explored.

#### 494 **Co-incorporated formulations: just a solid dispersion?**

495 Given the improvement of the formulation performance when HMPCAS was incorporated during the  
496 loading step rather than post-loading, it was important to rule out that a simple solid dispersion was  
497 formed directly, and that the silica in the formulation plays an important role in the dissolution  
498 enhancement. EDX indicates that the drug is localized in the silica particles and on the HPMCAS plate when  
499 the polymer is incorporated during the loading step (Figure 3, bottom panel), but is distributed freely  
500 throughout the entire sample when no silica is present (Figure 5). The results suggest that drug is confined  
501 within the mesoporous silica particles, which are in turn were immobilized in the polymer platelets when  
502 HMPCAS is incorporated in the drug loading step. Without the nanoconfinement effects of the silica  
503 (Ditzinger, 2018), the drug can re-crystallize, as observed in the XRPD (Figure 7). Ultimately, this resulted  
504 in the control sample showing no improvement in FaSSIF dissolution versus crystalline API (**Figure 6**).  
505 Furthermore, if a portion of the sample was able to remain amorphous in the polymer platelets, the  
506 absence of drug-polymer interaction (as shown in the solid-state NMR spectra) would reduce the  
507 precipitation inhibition effect of the polymer (**Figure 10**).

#### 508 **5. Conclusions**

509 A novel co-incorporated formulation of glibenclamide and the precipitation inhibitor, HMPCAS, onto  
510 mesoporous silica is described. By co-incorporating the precipitation inhibitor, the formulation  
511 significantly outperformed the commonly applied simple physical blend, regarding improved

512 supersaturation and dissolution in both single-medium FaSSIF and transfer dissolution assays.  
513 Furthermore, the co-incorporation approach allows the removal of a time-consuming and inefficient  
514 blending step. To provide a physical mechanistic basis is for the improved performance the co-  
515 incorporated formulation, a range of spectroscopic tools were utilized. It was concluded that the improved  
516 dissolution performance is a synergistic effect related to two key factors: formation of drug-polymer  
517 interactions in the solid state, and lack of release and premature precipitation under gastric conditions  
518 due to the immobilization of API-loaded silica particles within the enteric HPMCAS plates. Crucially, both  
519 of these properties are absent in a simple HPMCAS blend. Ultimately, the co-incorporation of precipitation  
520 inhibitors with the API on mesoporous silica formulations has the potential to improve both the process  
521 and formulation efficiency in the development of poorly soluble drugs.

## 522 **Acknowledgements**

523 The authors would like to thank Dr. Dieter Lubda, Dr Gudrun Birke and Dr. Finn Bauer for providing the  
524 Pardeck SLC® and for helpful and constructive discussions and feedback.

525

526 *This work has received funding from the European Union's Horizon 2020 research and innovation*  
527 *programme under grant agreement No. 674909 (PEARRL). [www.pearrl.eu](http://www.pearrl.eu)*

528

529

530

531

532

533

534

535

536

537

538

539

540 **Appendix 1: thermodynamic solubility values For glibenclamide**

*Appendix 1, Table 1. glibenclamide thermodynamic solubility values*

<i>Medium</i>	<i>Solubility (<math>\mu\text{g/mL}</math>)</i>
FaSSIF	$8.1 \pm 0.1$
SGF	<LOD*

541

542

543

544

545

546

547

548

549

550

551

552

553

554

555

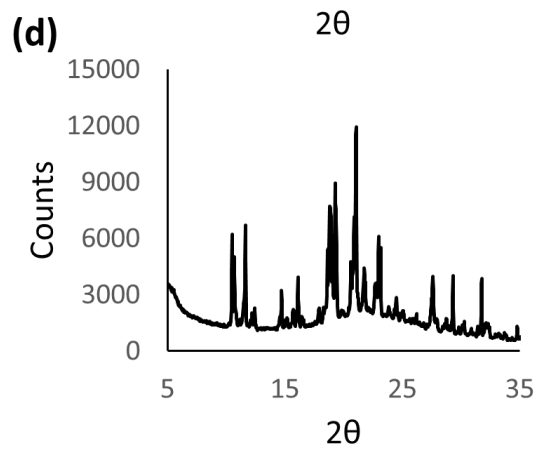
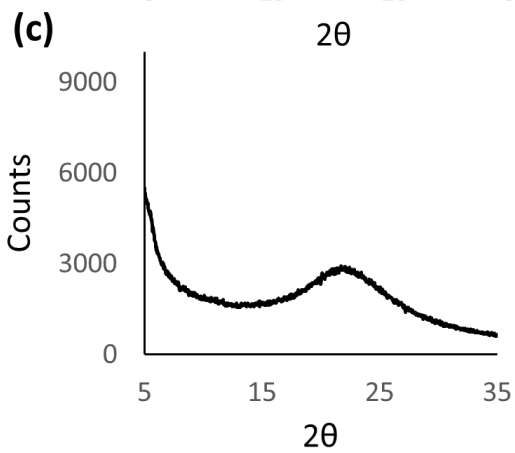
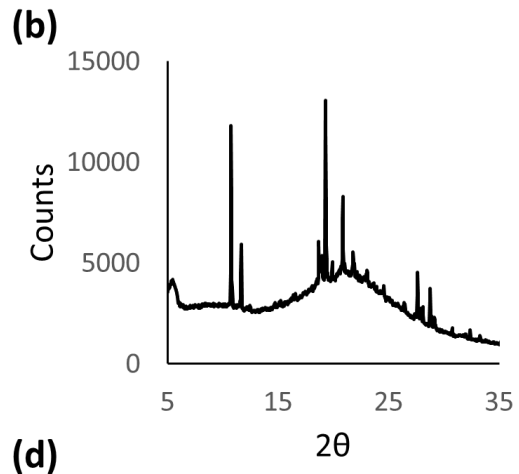
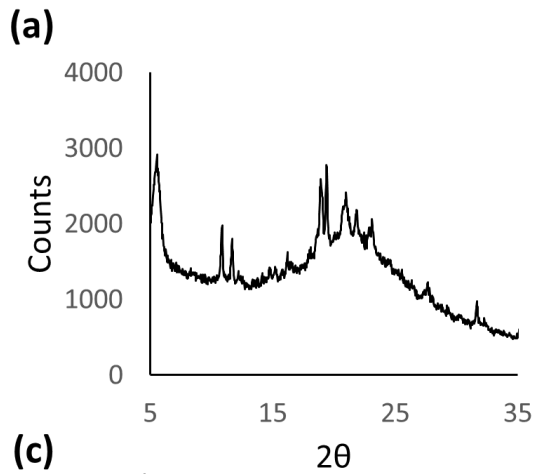
556

557

558

559





561

562 **Appendix 2.** XRPD patterns for post-FaSSIF dissolution residues for (a) glibenclamide loaded silica, (b)

563 glibenclamide loaded silica + HPMCAS blend, (c) glibenclamide and HPMCAS co-incorporated silica and (d)

564 glibenclamide and HPMCAS prepared by rotary evaporation (control)

565

566

567

568

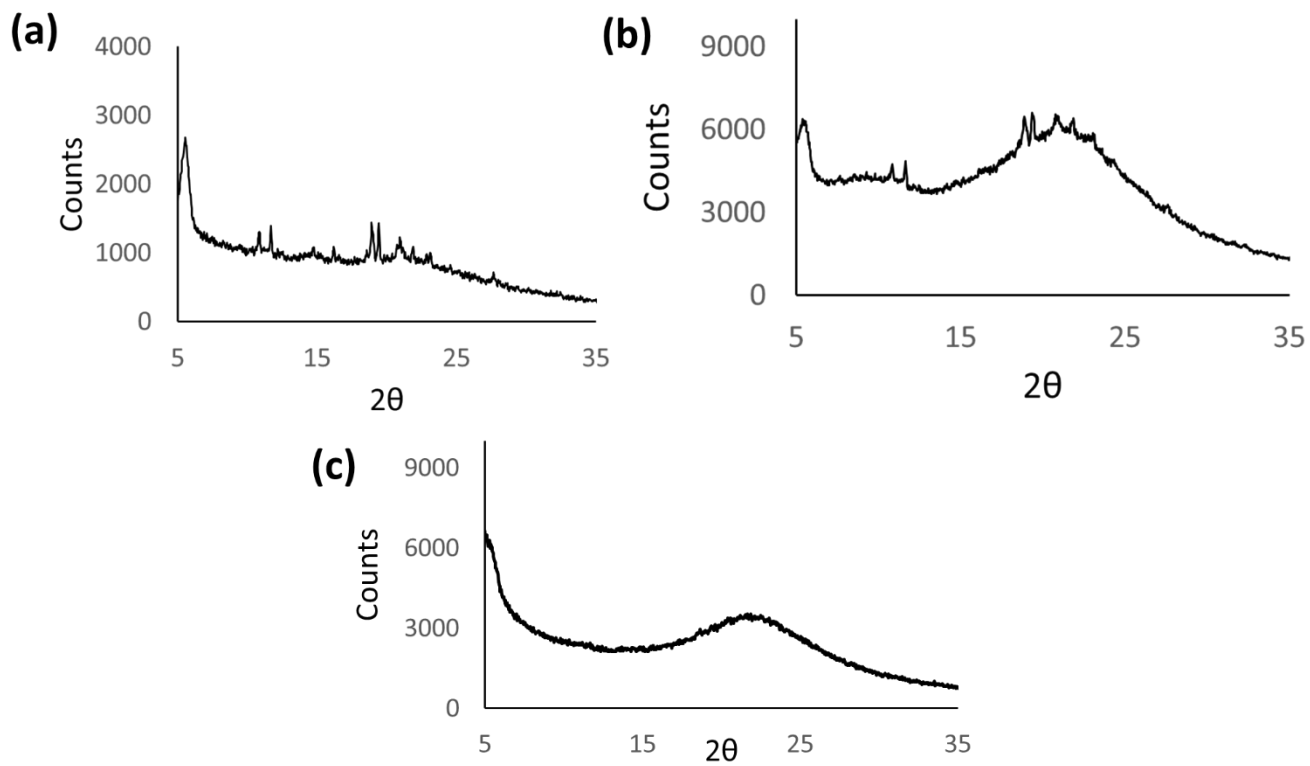
569

570

571

572

573 **Appendix 3: Post-SGF transfer dissolution XRPD patterns**



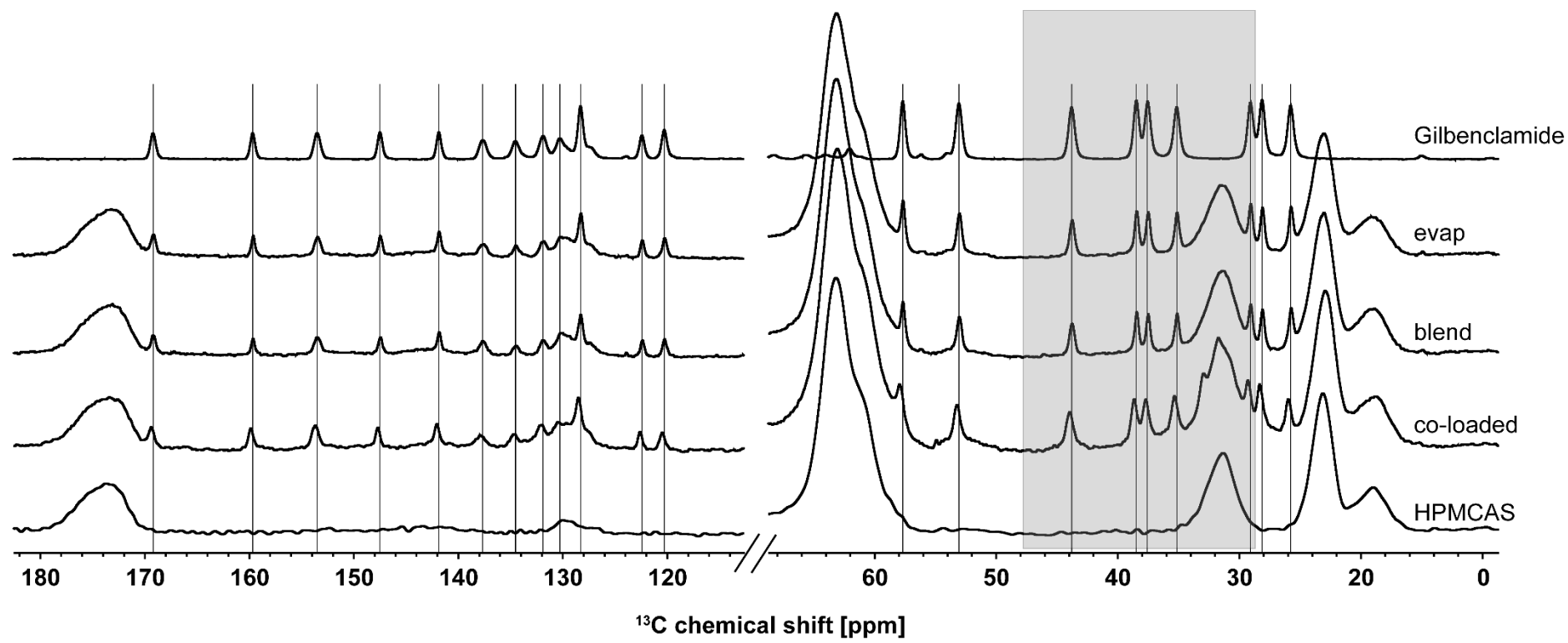
574

575

576 **Appendix 3.** XRPD patter for Glibenclamide loaded silica (a), glibenclamide loaded silica + HPMCAS blend

577 (b) and GB/HPMCAS co-incorporated silica (c) residues post-SGF transfer dissolution

**Appendix 4. SS-NMR spectra**



**Appendix 4.** Full solid-state NMR spectra for all samples showing peak shift in co-incorporated samples. The section highlighted corresponds to the section included in the main body of text.

## References

Amidon, G.L. et al. A theoretical basis for a biopharmaceutic drug classification: the correlation of in vitro drug product dissolution and in vivo bioavailability. *Pharm Res.* 12(3), (1995), 413-420.

Augustijns, P. and Brewster, ME. Supersaturating drug delivery systems: fast is not necessarily good enough. *J Pharm Sci.* 101(1), (2012), 7-9

Barbe, C. et al. Silica particles: A Novel Drug Delivery System. *Advanced Materials.* 2004, 16, pp.1959-1966.

Ditzinger, F. et al. Lipophilicity and hydrophobicity considerations in bio-enabling oral formulations approaches—a PEARRL review. *J Pharm Pharmacol.* Epub ahead of print

Fagerberg, J.H. et al. Ethanol Effects on Apparent Solubility of Poorly Soluble Drugs in simulated Intestinal Fluid. *Mol Pharm.* 9, (2012), 1942-1952. DOI: 10.1021/mp2006467

Hanada, M. et al. Enhanced Dissolution of a Porous Carrier-Containing Ternary Amorphous Solid Dispersion System Prepared by a Hot Melt Method. *J Pharm Sci.* 107(1), (2018), 362-371

Higashi, K. *et al.* Insights into Atomic-level Interaction between Mefenamic Acid and Eudragit® EPO in a Supersaturated Solution by HighResolution Magic-Angle Spinning NMR Spectroscopy. *Mol Pharm.* 11(1), 2014, 351-357

Knapik Stabilization of the amorphous ezetimibe by confining its dimension. *Mol. Pharm.* 2016. 13(4), 1308-1316.

Krishnaiah, Y.S.R. Pharmaceutical Technologies for Enhancing Oral Bioavailability of Poorly Soluble Drugs. *Journal of Bioequivalence and Bioavailability.* 2010, 2, 28-36.

Laine, AL. et al. Enhanced oral delivery of celecoxib via the development of a supersaturable amorphous formulation utilising mesoporous silica and co-loaded HPMCAS. *Int j pharm.* 512(1) (2016) 118-125. doi:10.1016/j.ijpharm.2016.08.034

Li, N. and Taylor, LS. Tailoring supersaturation from amorphous solid dispersions. *Journal of Controlled Release.* **279**, 2018, 114-125

Lipinski, C.A. Drug-like Properties and the Causes of Poor Solubility and Permeability. *Journal of Pharmacological and Toxicological Methods.* 2000, 44, 235-249.

Lipinski, C.A. Poor Aqueous Solubility- An Industry-Wide Problem in Drug Discovery. American Pharmaceutical Review. 2002, 5, 82-85

Loftsson, T. and Brewster, ME. Pharmaceutical applications of cyclodextrins: basic science and product development. J Pharm. Pharmacol. 62 (2010) 1607-1621. doi: 10.1111/j.2042-7158.2010.01030.x.

McCarthy, CA. et al. Mesoporous silica formulation strategies for drug dissolution enhancement: a review. Exp Op Drug Deliv. 13, (2016), 93-108. DOI: 10.1517/17425247.2016.1100165

Price, DJ. et al. Approaches to increase mechanistic understanding and aid in the selection of precipitation inhibitors for supersaturating formulations- A PEARL Review. J. Pharm. Pharmacol. 2018 (epub ahead of print). doi: 10.1111/jphp.12927.

Qiu, Y. and Lee, PI. Rational Design of Oral Modified-release Drug delivery systems. In: Developing Solid Oral Dosage Forms. Pharmaceutical Theory and Practice. (2017), 519-554

Sun, DD. And Lee, PI. Haste Makes Waste: The Interplay Between Dissolution and Precipitation of Supersaturating Formulations. AAPS J. 17(6), (2015), 1317-1326

Udea, K. et al. Equilibrium state at supersaturated drug concentration achieved by hydroxypropyl methylcellulose acetate succinate: molecular characterization using (1)H NMR technique. Mol Pharm. 12(4), (2015), 1097-104

Van Speybroeck, M. et al. Preventing release in the acidic environment of the stomach via occlusion in ordered mesoporous silica enhances the absorption of poorly soluble weakly acidic drugs. J Pharm Sci. 100(11), (2011), 4864-76

Van Speybroeck, M. et al. *Combined use of ordered mesoporous silica and precipitation inhibitors for improved oral absorption of the poorly soluble weak base itraconazole.* European Journal of Pharmaceutics and Biopharmaceutics. 75(3), 2010.

Warren, DB et al. Using polymeric precipitation inhibitors to improve the absorption of poorly water-soluble drugs: A mechanistic basis for utility. J Drug Targ. 18(10) (2010) 704-731. doi: 10.3109/1061186X.2010.525652

Zheng, W. et al. Selection of Oral Bioavailability Enhancing Formulations during Drug Discovery. Drug Development and Industrial Pharmacy. 2012, 38(2), 235-247.